DOI: 10.26599/FSHW.2026.9250973

Contents lists available at SciOpen

Food Science and Human Wellness

journal homepage: https://www.sciopen.com/journal/2097-0765

China Food Publishing Co.

Human milk oligosaccharide 2'-fucosyllactose and lacto-n-neo-tetraose attenuate early-weaning-induced intestinal barrier dysfunction in mice

Ru Chen[1,2,3], Yu-ling Zhao[1,2,3], Yong-chang Zhou[2,3], Lu Jiang[2,3]*, Wei Cai[1,2,3]*

[1]*Department of Pediatric Surgery, Xinhua Hospital, School of Medicine, Shanghai Jiao Tong University, Shanghai, China.*

[2]*Shanghai Key Laboratory of Pediatric Gastroenterology and Nutrition, Shanghai, China.*

[3]*Shanghai Institute for Pediatric Research, Shanghai, China.*

ABSTRACT: Breastfeeding is universally acknowledged as pivotal for optimal infant development, yet early weaning remains a common choice among young mothers. Accumulating evidence indicates that early weaning disrupts intestinal development and induces gut dysbiosis; however, the impact of human milk oligosaccharides (HMOs) on intestinal function remains unclear. In this study, we aimed to investigate the effects of two major HMOs, 2'-fucosyllactose (2'-FL) and lacto-N-neotetraose (LNnT), on intestinal barrier function and their underlying mechanisms. Two-week-old mice were weaned and supplemented with 2'-FL, LNnT, or a combination of both (referred to as 2'-FL/ LNnT) for one week while being maintained on a liquid diet to support normal growth. We observed that both 2'-FL and LNnT, individually and in combination, alleviated early-weaning-induced gut barrier damage in the jejunum. RNA sequencing and subsequent validation revealed that the 2'-FL/LNnT combination activated the AMPK/SREBPs signaling pathway more robustly than either one alone. Interestingly, in vitro experiments demonstrated that HMOs did not directly affect the AMPK/SREBPs signaling. By 16S rDNA sequencing, we found that early weaning significantly reduced the microbial diversity, which was restored only in the 2'-FL/LNnT group. Finally, through antibiotic treatment and fecal microbiome transplantation (FMT) experiments, we confirmed that the protective effects of 2'-FL/LNnT on intestinal barrier function were gut microbiota-dependent. Collectively, these findings suggest that 2'-FL and LNnT protect against gut barrier dysfunction in early-weaned mice and may offer novel therapeutic strategies.

Keywords: early weaning, gut barrier, microbiota, 2'-fucosyllactose, lacto-N-neotetraose

1. Introduction

The World Health Organization (WHO) advocates exclusive breastfeeding for the first six months of life, followed by continued breastfeeding alongside appropriate complementary foods up to two years of age. Early weaning (EW) remains a pressing global public-health challenge, linked to heightened lifetime risks of numerous diseases. Globally, only 37% of infants are exclusively breastfed for the full first six months, leaving the majority without this vital nutritional foundation [1]. Extensive research has demonstrated that EW contributes to the pathogenesis of multiple adverse health outcomes, including allergies [2], obesity [3], malnutrition [4], severe respiratory infections [5], and impaired oral motor development [6]. Notably, early

***Corresponding author**
Lu Jiang; jianglu@xinhuamed.com.cn.Wei Cai; caiw1978@163.com.

Received 26 July 2025
Received in revised from 21 October 2025
Accepted 25 December 2025

weaning has been strongly associated with gastrointestinal pathogenesis, including increased risks of diarrhea morbidity and mortality in HIV-exposed uninfected infants, as well as elevated intestinal permeability and inflammatory markers in infants with genetic susceptibility to type 1 diabetes [7-9]. Accumulating evidence indicates that EW leads to compromised gut barrier, characterized by accelerated microbial colonization dynamics [10], compromised mucosal integrity [11], increased intestinal permeability, and dysregulated expression of tight junction proteins [12]. Although the adverse consequences of EW are well documented, the precise mechanisms underlying its detrimental impact on gut barrier remain elusive.

Human milk is considered the best source of nutrition for infants, offering vital nutrients in exquisitely balanced proportions during the first six months of life. Beyond its fundamental constituents—water, carbohydrates, fats, proteins, vitamins, and minerals—it delivers various bioactive components, such as oligosaccharides, immune factors, growth factors, and hormones [13]. Human milk contains approximately 7% carbohydrates, of which lactose accounts for about 80% and human milk oligosaccharides (HMOs) make up the remaining 20% [14]. 2'-fucosyllactose (2'-FL) and lacto-N-neotetraose (LNnT) are two abundant HMOs, with concentrations ranging from 0.7 to 3.4 g/L for 2'-FL and 0.3 to 1.0 g/L for LNnT. Collectively, they occupy up to 40% of the total HMOs in human milk [15]. Clinical studies have revealed that infant formulas supplemented with 2'-FL and LNnT are safe and conferred vital health benefits such as reduced incidence of bronchitis and respiratory tract illnesses [16-18]. Moreover, the infant formula supplemented with 2'-FL and LNnT has been found to positively modulate the gut microbiome by increasing the relative abundance of *Bifidobacterium* and *Lactobacillus*, while drastically reduced the abundance of *Clostridium*, *Veillonella*, and *Eubacterium* in infants [18, 19]. In preclinical studies, in vivo and in vitro studies have proved that 2'-FL and LNnT showed prebiotic, antibacterial, antiviral, and immunomodulatory properties, while also modulating the glycome (such as intestinal epithelial glycocalyx) of the host's epithelial cell surface [20, 21]. Under pathological conditions, 2'-FL could restore the intestinal mucosal barrier in a mouse model of ulcerative colitis by suppressing the palmitoylation and phosphorylation of signal transducer and activator of transcription 3 (STAT3) [22]. Additionally, LNnT stimulated intestinal epithelial growth and maturation during the early life of mice [23]. These positive outcomes are strongly related to the beneficial modulation of infant gut microbiota development [24]. Therefore, while existing evidence highlights the beneficial roles of HMOs in gut microbiota modulation, their specific mechanisms in the context of EW remain unknown.

In this study, we developed a mouse model of EW to systematically investigate the effects of 2'-FL, LNnT and the combination of both (referred to as 2'-FL/LNnT) on intestinal barrier function and gut microbiota composition. Specifically, we aimed to determine whether these HMOs exert their beneficial effects through gut microbiota modulation, and to characterize the underlying molecular mechanisms.

2. Materials and Methods

2.1 Establishment of the EW mice model

C57BL/6J mouse pups were weaned at postnatal day 14 (PND 14) as previously described [25]. Briefly, dams were separated from their litters for 18 hours (3:00 pm–9:00 am) on PND 14, followed by a 6-hour

reunion period (9:00 am–3:00 pm) to facilitate adaptation. Following this interval, pups were permanently weaned and supplemented with an AIN-93G liquid diet to maintain growth until PND 21 [26].

2.2 Animal study on HMO supplementation

At postnatal day 14 (PND 14), mouse pups were randomly divided into five experimental groups: (1) Normal suckling; (2) EW group (early weaning at PND 15); (3) EW+2'-FL/ LNnT (2 g/L 2'-FL + 0.5 g/L LNnT) group; (4) EW + 2'-FL (2 g/L) group; and (5) EW + LNnT (0.5 g/L) group. Body weight and food intake were monitored daily. 2'-FL and LNnT (purity > 92%) were donated by dsm-firmenich (Kaiseraugst, Switzerland). All animals were euthanized at PND 21. Blood, intestine, and fecal samples were collected for further analysis.

2.3 Pharmacological inhibition of the AMPK signaling pathway

Littermate pups were randomly assigned to three groups: (1) EW + vehicle (5% DMSO); (2) EW + 2'-FL/LNnT; (3) EW + 2'-FL/LNnT + Compound C (CC). CC was administered intraperitoneally at 10 mg/kg once daily for 7 days [27]. Body weight was recorded daily. On day 7 post-weaning, mice were euthanized, and jejunal tissues were collected for analysis.

2.4 Antibiotic (ABX) treatment and fecal microbiota transplantation (FMT)

Following EW, mice were randomly divided into 4 groups (n = 5 per group): (1) Suckling group; (2) EW model group; (3) EW + 2'-FL/LNnT group; and (4) EW + ABX + 2'-FL/LNnT group. To deplete the gut microbiota, mice received twice-daily oral gavage of a broad-spectrum antibiotic cocktail consisting of ampicillin (200 mg/kg/day), neomycin sulfate (200 mg/kg/day), metronidazole (200 mg/kg/day), and vancomycin hydrochloride (100 mg/kg/day) for five consecutive days. Following microbiota depletion, animals were supplemented with a mixture of 2'-FL and LNnT for 7 days.

The FMT experiments were conducted as previously described [28], using mice from either the EW group or the EW + 2'-FL/LNnT group as donors, with EW mice as recipients. For FMT preparation, 1 g of feces was homogenized in PBS (0.125 g/mL), followed by centrifugation at 500 g for 3 min at 4 ℃. Fresh fecal microbiota suspensions were freshly prepared to ensure bacterial viability.

2.5 Cell culture and treatment

Caco-2 cells were cultured at 37℃ in a humidified atmosphere of 5% CO_2 in Dulbecco's modified Eagle medium (DMEM) supplemented with 10% fetal bovine serum (Gibco, USA), 1% penicillin-streptomycin (100×) (Servicebio, Wuhan, China). 2'-FL (2.4 g/L), LNnT alone (0.6 g/L), a combination of 2'-FL and LNnT, and fecal supernatants from mice in the EW (Weaned-M) or 2'-FL/LNnT (2'-FL/LNnT-M) groups were co-cultured with Caco-2 cells. After 24 hours, cellular proteins were extracted for further analysis.

2.6 RNA extraction and real-time qPCR

Total RNA was extracted from intestinal tissue using Trizol reagent. RNA quality was assessed by determining concentration and purity using a NanoDrop spectrophotometer (Thermo Fisher Scientific, USA). The RNA was reverse transcribed into cDNA and qPCR was performed with SYBR Green Master Mix

(Yeasen, Shanghai, China) following the manufacturer's instructions. Gene expression was quantified using the 2−ΔΔCt method, with β-actin as the internal control. Primer sequences for qPCR are listed in Table 1.

Table 1. Primer sequences for qPCR

Gene Name	Forward Sequence	Reverse Sequence
Actb	GGCTGTATTCCCCTCCATCG	CCAGTTGGTAACAATGCCATGT
Tjp1	ACTCCCACTTCCCCAAAAAC	CCACAGCTGAAGGACTCACA
Cldn1	CGATGAGGTGCAGAAGATGA	CCAGTGAAGAGAGCCTGACC
Ocln	GTATAAGTCACCGCCTCTG	ACTCTTCGCTCTCCTCTC
Cdh1	GTCACTGACACCAACGATAATCCT	TTTCAGTGTGGTGATTACGACGTTA
Tnfa	GGTGCCTATGTCTCAGCCTCTT	GCCATAGAACTGATGAGAGGGAG
Ifng	ATGAACGCTACACACTGCATC	CCATCCTTTTGCCAGTTCCTC
Srebf1	CAGTCTAGCAGACGGAACGG	TCCTTCATATGTGTAGGTCTGGA
Fasn	CCGTGAGACCCACAACAGAA	GCCATGAACTGGGAGGCTAT
Acc1	GGCTCCAAGTCCCATTGTCA	AATGTACGTCCACAACGGCT
Scd1	GAGGCCACCATCATGACGAA	GGTGACCAGGGTCTTGACAT
16S rRNA	GTGSTGCAYGGYTGTCGTCA	ACGTCRTCCMCACCTTCCTC
A. muciniphila	AGAGGTCTCAAGCGTTGTTCGGAA	TTTCGCTCCCCTGGCCTTCGTGC

2.7 Protein extraction and western blot analysis

Proteins were extracted from intestinal tissue or Caco-2 cells using cell lysis buffer containing protease and phosphatase inhibitors. Proteins were subjected to 10% sodium dodecyl sulfate–polyacrylamide gel electrophoresis and electroblotted to nitrocellulose membranes. Antibodies against CLAUDIN-1, OCCLUDIN, AMPK, p-AMPK, and β-ACTIN were purchased from Cell Signaling Technology (Danvers, MA). Antibodies against ZO-1 and SREBP1/2 were purchased from Bioss Biotechnology Co., Ltd. (Beijing, China). Anti-rabbit IgG and anti-mouse IgG secondary antibodies were purchased from Cell Signaling Technology (Danvers, MA).

2.8 Intestinal permeability assay

Intestinal permeability was assessed using FITC-dextran (4 kDa) as previously described [29]. After an overnight fast, mice were orally gavaged with FITC-dextran dissolved in PBS (600 mg/kg body weight). Blood was collected from the orbital plexus 4 h post-gavage under anesthesia. Serum was obtained by centrifugation and diluted. FITC-dextran levels were quantified fluorometrically (excitation 485 nm, emission 520 nm) using a standard curve for calibration.

2.9 RNA sequencing

RNA-seq libraries were prepared from total RNA, with ribosomal RNA removed, and sequenced on the Illumina NovaSeq™ 6000 platform (LC Bio Technology Co Ltd., Hangzhou, China). Raw reads were trimmed using Cutadapt [30] and aligned to the mouse reference genome (GRCm39/mm39) with HISAT2 [31]. Differentially expressed genes (DEGs) were identified using DESeq2 [32], with a fold change (FC) ≥ 1.5 and false discovery rate (FDR) < 0.05 considered significant, followed by KEGG pathway analysis [33]. Upstream regulator analysis was conducted on differentially expressed genes using Ingenuity Pathway Analysis (IPA) software v01-23-01. An absolute Z-score ≥2 is considered significant. Sequence data were registered at NCBI

under BioProject PRJNA1295196. The accession number for RNA-seq data reported in this study was GEO: GSE303393.

2.10 DNA Extraction and 16S rDNA sequencing

Bacterial DNA was extracted from mouse stool samples using the TIANamp stool DNA kit (TIANGEN, Beijing, China). The 16S rDNA sequencing was performed as previously described [34]. Briefly, the V3-V4 region of the 16S rDNA were amplified and sequenced on the Illumina Miseq platform (Majorbio Co., Ltd., Shanghai, China). Raw sequence reads have been deposited in the NCBI SRA with BioProject PRJNA1292824.

2.11 Fecal SCFA measurement

SCFAs were quantified using a triple-quadrupole gas chromatograph mass spectrometer (Suzhou PANOMIX Biomedical Tech Co., Ltd). Briefly, 300 mg of mouse feces were homogenized in 100 μL of pre-cooled phosphate buffer using zirconia steel beads. Subsequently, 1 mL of ethyl acetate was added, and the mixture was thoroughly vortexed. After centrifugation at 3,000 r/min for 10 min at 4 ℃, the supernatant was collected and passed through a 0.22-μm organic membrane filter prior to GC-MS analysis.

2.12 Statistical analysis

Statistical analyses were performed using GraphPad Prism 9.0 software, and the results are expressed as the mean ± s.e.m. One-way analysis of variance (ANOVA) followed by Tukey's multiple comparison tests were used for statistical analysis of differences among three or more experimental groups, with $P < 0.05$ considered statistically significant.

3. Results

3.1 Effects of HMOs on the intestinal development in EW mouse model

To assess the effects of HMOs on growth and intestinal development in EW, we established a modified mouse model of EW based on a previous publication [24]. The experimental design is shown in Fig. 1A. Overall, the body weight and food intake showed no significant differences among the groups during the 7-day treatment period (Fig. 1B-D). Similarly, small intestinal length did not differ significantly across groups (Fig. 1E-F). Histological analysis by H&E staining revealed no notable differences in villus height (Fig. 1G) or crypt depth (Fig. 1H) between groups. Next, we investigated the effects of HMOs on ileum and colon. By H&E staining, we found that both ileum and colon showed conserved villus architecture and epithelial integrity mucosal organization without observable structural damage (Fig. S1A, Fig. S2A).

As the jejunum serves as the primary site for nutrient sensing and absorption, we next examined jejunal ultrastructural changes using transmission electron microscopy (TEM). Notably, both the length and the area of jejunal microvilli were significantly reduced in the EW group compared with the suckling group, and these morphological alterations were effectively restored by either LNnT or 2'-FL/LNnT (Fig. 1I-J). Since EW predominantly affects jejunal morphology, we subsequently investigated how HMOs modulate jejunal barrier function under EW conditions.

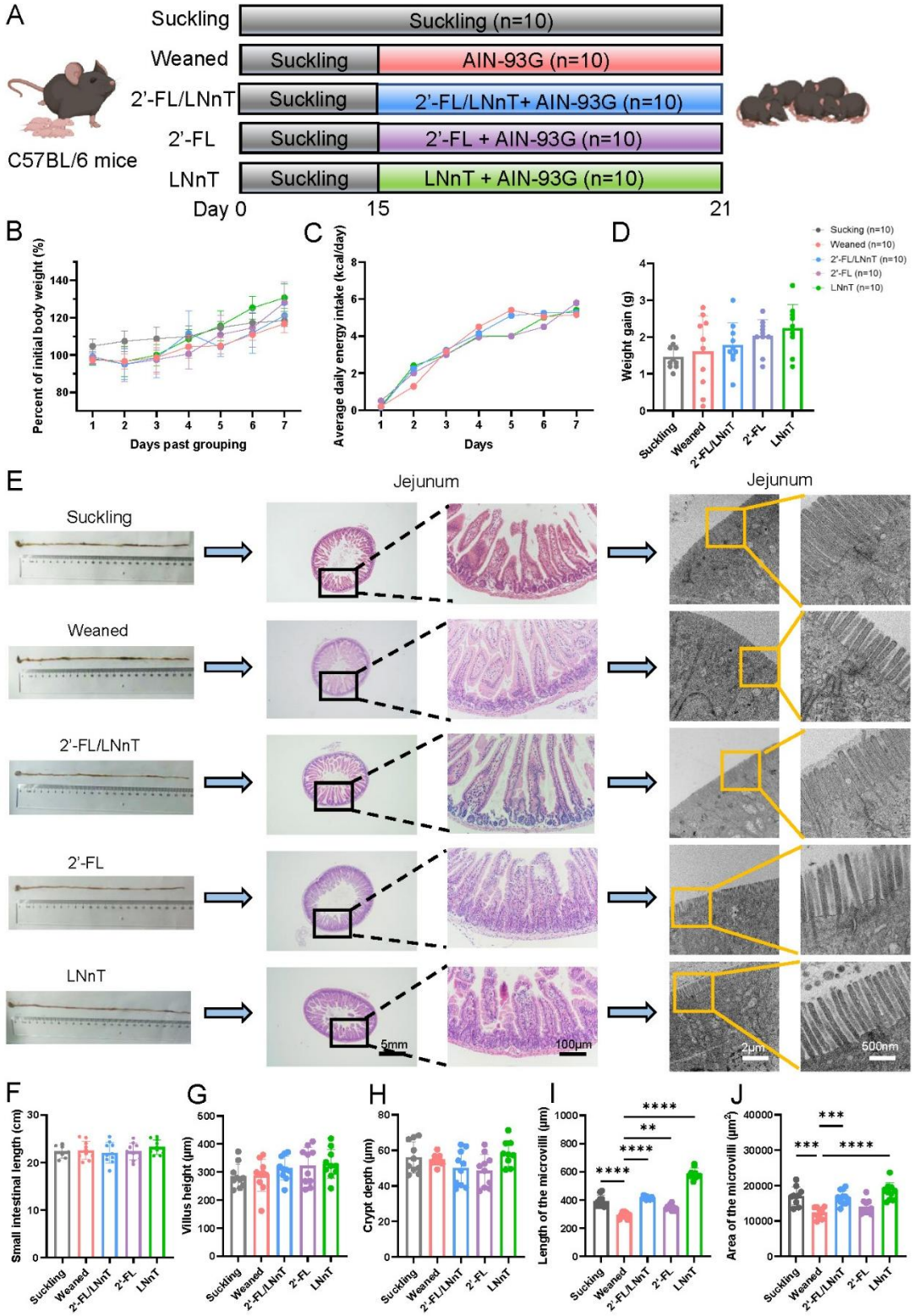

Figure 1. Effects of HMOs on intestinal development in a mouse model of early weaning (EW). Mice were divided into five groups: (1) Normal suckling; (2) EW group; (3) EW + 2'-FL/LNnT (2'-FL + LNnT) group; (4) EW + 2'-FL group; and (5) EW + LNnT group. (A) Animal experimental design. (B) Body weight was monitored daily during the experiment. (C) The average daily energy intake (kcal/day) was measured during the experiment. (D) The weight gain was determined at the end of the experiment. (E) Representative images of small intestines, H&E staining, and transmission electron microscopy (TEM) on jejunum of mice from the five groups. (F-H) The length of small intestine, villous height, and crypt depth were determined. (I-J) Length of the microvilli (μm) and area of the microvilli (μm^2). n =10 per group. $^{**}P < 0.01$, $^{***}P < 0.001$, $^{****}P < 0.0001$.

3.2 HMOs improved intestinal barrier integrity in EW mice

To study the effect of HMOs on the integrity of the jejunal epithelium in EW mice, we conducted the FITC-dextran assay and measured the expression of tight junctions-related genes by qPCR. We found that serum of EW mice exhibited higher absorption of fluorescence relative to the suckling group, reflecting a leaky gut, which was reduced in the LNnT or 2'-FL/LNnT groups (Fig. 2A). Compared with the suckling group, the EW group exhibited significantly suppressed mRNA levels of *Tjp1* (encodes ZO-1), *Ocln*, and *Cldn1*. This suppression was effectively restored by the combined supplementation of 2'-FL/LNnT. In contrast, 2'-FL supplementation only elevated *Tjp1* expression, while LNnT alone specifically restored the expression of both *Tjp1* and *Cldn1* (Fig. 2B). Consistently, the protein levels of CLAUDIN-1 and OCCLUDIN were significantly decreased in the jejunum of the EW group, while HMO supplementation upregulated their expression. The expression of ZO-1 showed a similar trend, although it did not reach statistical significance (Fig. 2C-D). As expected, the expression levels of tight junction-related genes and proteins remained unchanged in the ileum (Fig. S1B-E) and colon (Fig. S2B-E).

TEM analysis demonstrated EW-induced damage to intercellular junctions (red arrows) and mitochondrial swelling (blue arrows) (Fig. 2E-F). These morphological defects were markedly attenuated by HMO treatment, with the 2'-FL/LNnT group showing the most pronounced restoration of microvillus structure and cellular organization. Taken together, these findings demonstrate that EW induces jejunal epithelial injury, while HMO supplementation exerts protective effects.

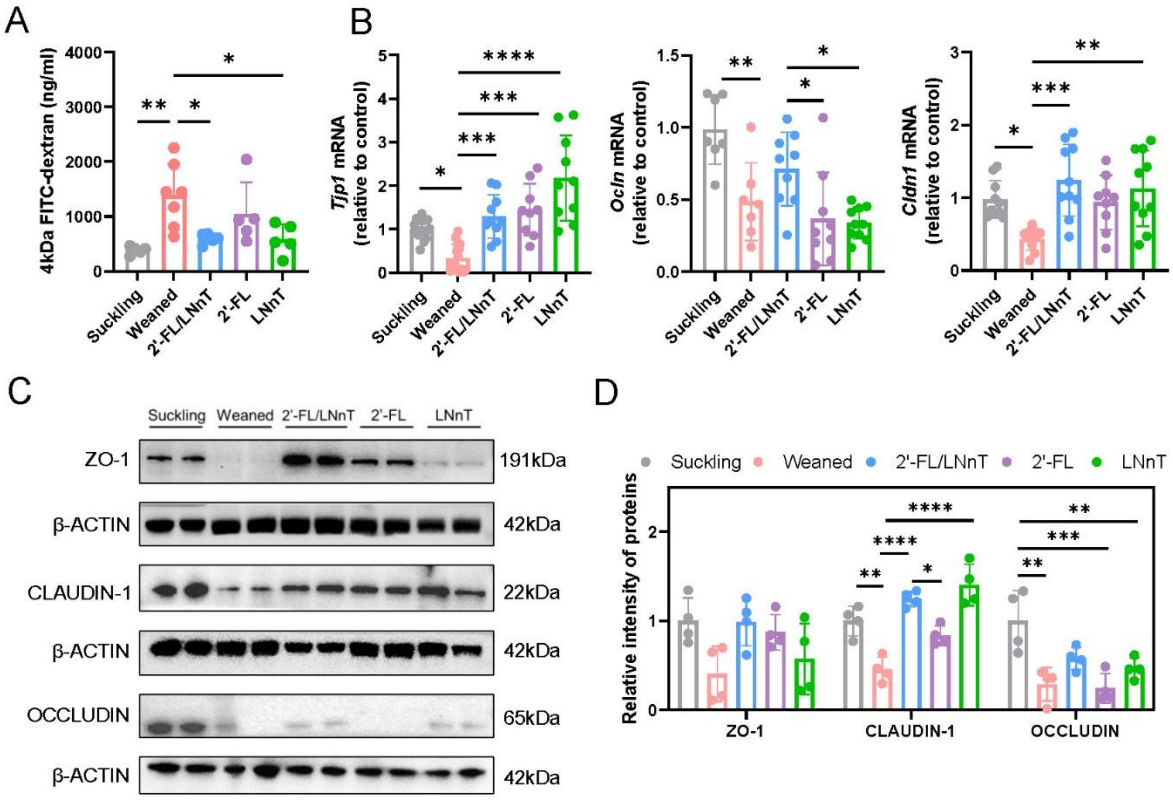

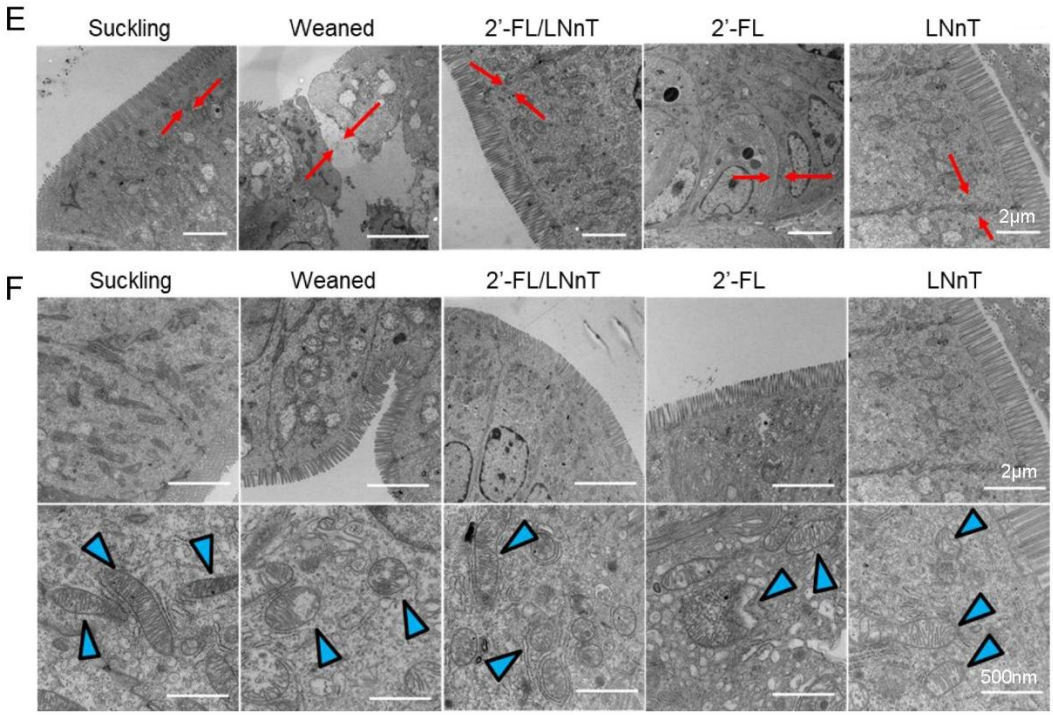

Figure 2. HMOs protect against early weaning (EW)-induced intestinal barrier dysfunction in mice. Mice divided into five groups: (1) Normal suckling; (2) EW group; (3) EW + 2'-FL/LNnT group; (4) EW + 2'-FL group; and (5) EW + LNnT group. (A) Concentrations of FITC-dextran in serum. (B) The mRNA levels of *Tjp1*, *Ocln*, and *Cldn1* in the jejunum. (C-D) Protein levels of ZO-1, CLAUDIN-1, and OCCLUDIN determined by western blotting (n =4 per group). (E-F) Representative images of transmission electron microscopy (TEM) for jejunum epithelium in all groups. Red arrows indicate the intercellular space of the epithelial cells. Blue arrows indicate mitochondria. n =10 per group. **P* < 0.05, ***P* < 0.01, ****P* < 0.001, *****P* < 0.0001.

3.3 2'-FL/LNnT regulate gut barrier function through the AMPK/SREBPs signaling pathway

To investigate the molecular mechanisms underlying HMO function in EW, we performed RNA-seq analysis on jejunal tissues. IPA revealed that the synthesis of lipid, cholesterol biosynthesis, and metabolism of cholesterol pathways was activated in the EW group, with SREBF1 and SREBF2 identified as key transcriptional regulators (Fig. 3A). Upstream regulator analysis of the DEGs revealed 27 transcriptional regulators, of which 23 were activated (top 10 shown in the graph) and 4 were inhibited (Fig. 3B). When we compared the suckling group vs. the EW group and the EW vs. the 2'-FL/LNnT group, we found that the AMPK signaling pathway was significantly enriched in both datasets (Fig. 3C-D).

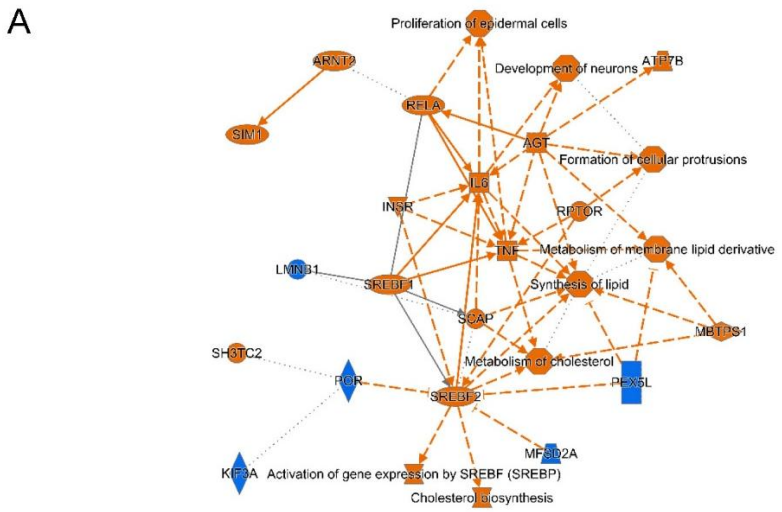

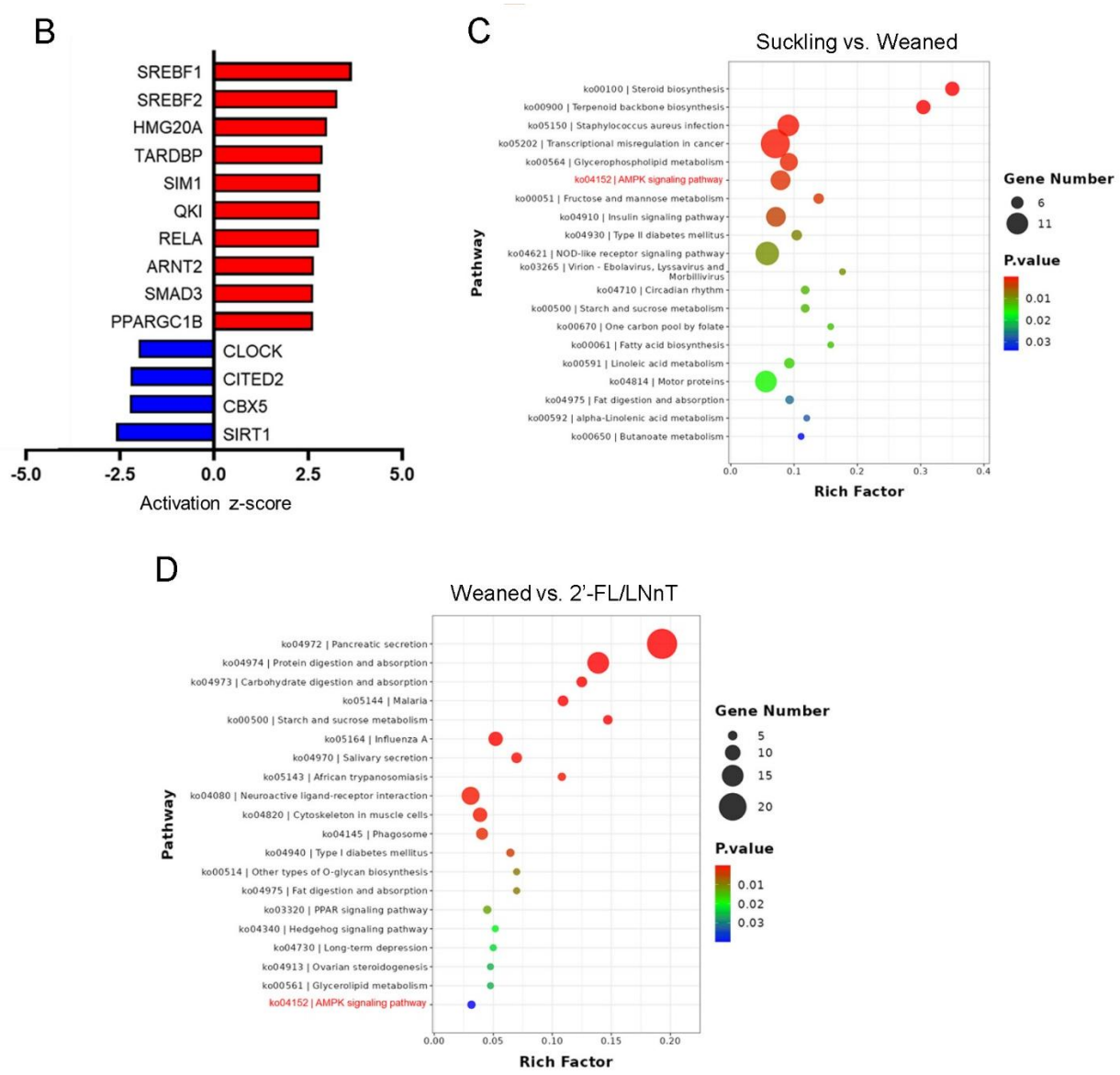

Figure 3. HMOs regulate the intestinal barrier function through activating the AMPK/SREBPs signaling pathway. Mice divided into three groups: (1) Normal suckling; (2) EW group; and (3) EW + 2'-FL/LNnT group. (A) Graphical summary of comparison between the early weaning (EW) and the suckling groups by Ingenuity Pathway Analysis (IPA). (B) Bar graph showing the top 10 and 4 up-and downstream transcription regulators predicted by IPA. (C-D) Pathway enrichment analyses of differentially expressed genes based on the KEGG database. Comparisons were made between sucking vs. EW (C) and EW vs. 2'-FL/LNnT (D).

Previous research suggest that AMPK is a crucial regulator of cellular energy balance, metabolism, and stress responses [35], and it upregulates the expression of epithelial tight junctions [36]. Given that SREBF is a downstream target of AMPK [37], we next performed Western blot on AMPK and SREBP1/2. Our findings revealed a significant decrease in phosphorylated AMPK (p-AMPK) levels in the EW group. While 2'-FL treatment significantly restored AMPK phosphorylation, LNnT alone showed no significant effect. Interestingly, the 2'-FL/LNnT demonstrated synergistic enhancement of p-AMPK beyond individual treatments (Fig. 4A-B). Consistently, EW led to a significant upregulation of SREBP1/2 expression, which were inhibited by 2'-FL/LNnT (Fig. 4C-D). Correspondingly, mRNA levels of SREBP1 downstream targets (*Fasn*, *Scd1*, *Acc1*) mirrored these regulatory patterns (Fig. 4E).

To determine whether 2'-FL or LNnT directly phosphorylates AMPK, we treated Caco-2 cells with 2'-FL, LNnT, 2'-FL/LNnT, fecal supernatant from EW mice, and fecal supernatant from EW mice supplemented with 2'-FL/LNnT. We found that neither 2'-FL nor LNnT phosphorylated AMPK (Fig. 4F-G). These data suggests that AMPK activation was mediated by microbiota metabolites derived from 2'-FL/LNnT-treated mice, rather than by direct activation by the 2'-FL/LNnT themselves.

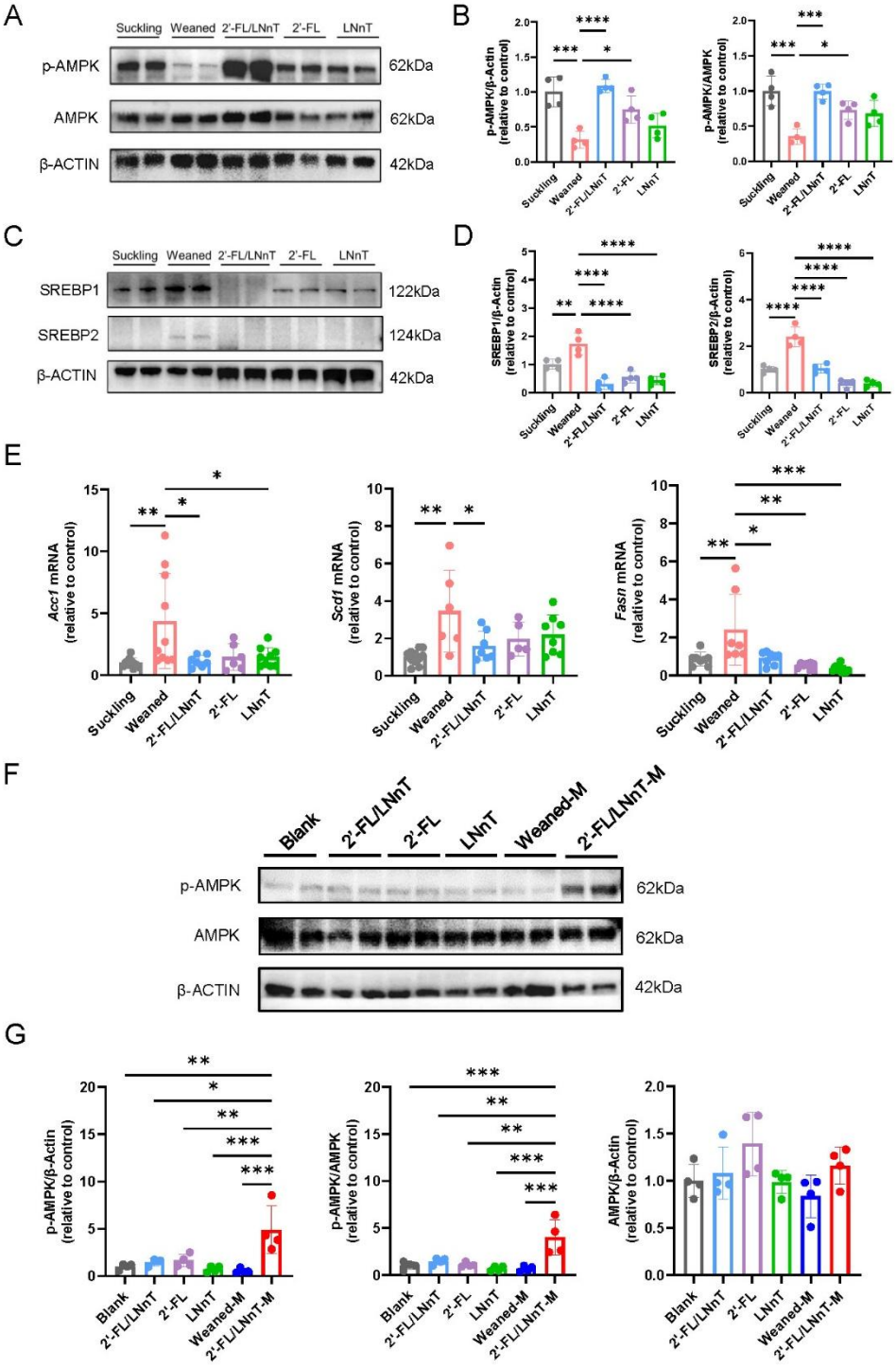

Figure 4. HMOs activate the AMPK/SREBPs signaling pathway in early weaning (EW) mice. Mice divided into five groups: (1) Normal suckling; (2) EW group; (3) EW + 2'-FL/LNnT (2'-FL + LNnT) group; (4) EW + 2'-FL group; and (5) EW + LNnT group. (A-D) Protein levels of p-AMPK, AMPK, SREBP1, and SREBP2 in the jejunum determined by western blotting (n =4 per group). (E) The mRNA levels of *Fasn*, *Scd1*, and *Acc1* in the jejunum, as assessed by qPCR. (F-G) Western blotting analysis of p-AMPK and AMPK in Caco-2 cells treated with control, 2'-FL/LNnT, 2'-FL, LNnT, fecal supernatant from EW mice, and fecal supernatant from EW mice supplemented with 2'-FL/LNnT. **P* < 0.05, ***P* < 0.01, ****P* < 0.001, *****P* < 0.0001.

3.4 2'-FL/LNnT protect against EW-induced intestinal barrier injury through AMPK signaling pathway

To further validate that 2'-FL/LNnT exert their effects via AMPK pathway activation, we treated EW mice with 2'-FL/LNnT in the presence or absence of the AMPK inhibitor Compound C (CC). Compared with the EW group, the 2'-FL/LNnT + vehicle group exhibited a significant increase in jejunal villus length, which was abolished by CC treatment (Fig. 5A-B). Interestingly, the crypt length was decreased in the 2'-FL/LNnT + CC group compared with the 2'-FL/LNnT + vehicle group (Fig. 5C).

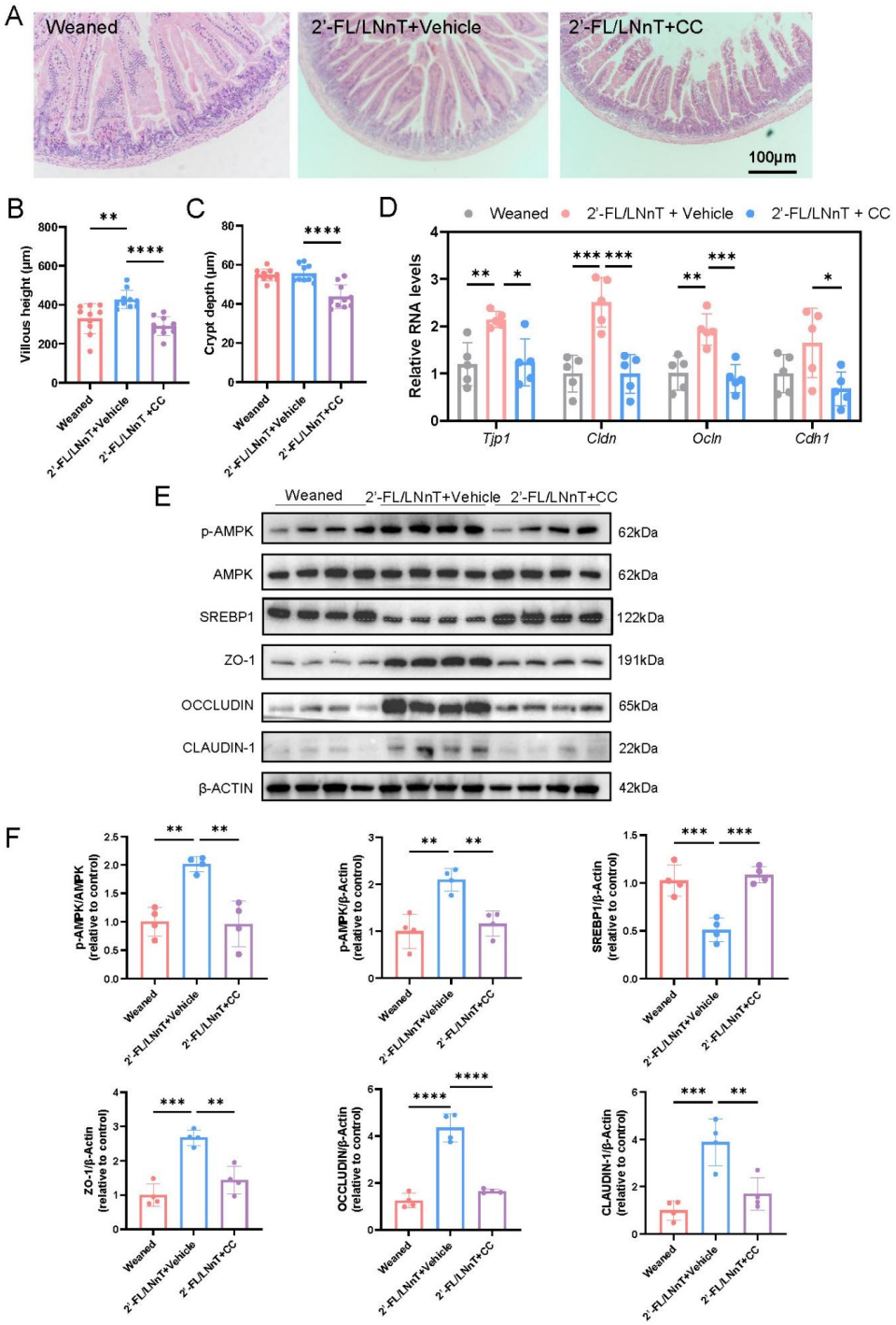

Figure 5. The effects of AMPK inhibitor Compound C (CC) on the intestinal barrier integrity in early weaning (EW) mice. (A) Representative images of H&E staining on jejunum in the EW, 2'-FL/LNnT + Vehicle group, and the 2'-FL/LNnT + CC groups. (B) Villous height and (C) crypt depth were determined in mice (n = 5 per group). (D) The mRNA levels of *Tjp1*, *Ocln*, and *Cldn1* in the jejunum, assessed by qPCR. (E-F) The protein level of p-AMPK, AMPK, SREBP1, ZO-1, OCCLUDIN, and CLAUDIN-1, as determined by western blotting. **P* < 0.05, ***P* < 0.01, ****P* < 0.001, *****P* < 0.0001.

Moreover, qPCR analysis revealed significant upregulation of tight junction-related genes (*Tjp1*, *Cldn*, *Ocln*, and *Cldn1*) in the 2'-FL/LNnT + vehicle group, which were reversed by CC treatment (Fig. 5D). Western blot analysis confirmed that CC treatment reversed the 2'-FL/LNnT-induced upregulation of p-AMPK, ZO-1, Occludin, and Claudin-1, while conversely increasing SREBP1 expression (Fig. 5E-F). These findings suggest that 2'-FL and LNnT protect against EW-induced intestinal barrier dysfunction by activating AMPK/SREBPs.

3.5 2'-FL/LNnT restored the microbial diversity in EW mice

Previous studies suggest that EW induces gut dysbiosis in piglet models [10]. To examine whether 2'-FL or LNnT affect the gut microbiota, we performed 16S rDNA sequencing using fecal samples. The Shannon index showed a decreasing trend in EW mice compared with the suckling group, which was reversed by 2'-FL/LNnT supplementation (Fig. 6A). PCA plot revealed a distinct separation between the EW model group and the suckling group, which was reversed by 2'-FL/LNnT supplementation (Fig. 6B). The Microbial Dysbiosis Index (MDI), a quantitative indicator of gut microbiota imbalance, was significantly higher in the EW group relative to the suckling group. However, supplementation with 2'-FL, LNnT, or a combination of 2'-FL/LNnT did not lead to any further changes in MDI scores compared with the EW group (Fig. 6C). Interestingly, neither the 2'-FL nor the LNnT alone affected the microbial diversity (Fig. 6A-C), indicating that only the combined 2'-FL/LNnT are required to ameliorate EW-induced gut dysbiosis. At the phylum level, the EW group exhibited a lower Bacillota (formerly Firmicutes)-to-Bacteroidota (formerly Bacteroidetes) ratio than the suckling group. Although 2'-FL/LNnT supplementation significantly counteracted this reduction, neither 2'-FL nor LNnT treatment led to a significant elevation in the ratio (Fig. 6D-E). At the genus level, we found that the *Akkermansia* and *Paramuribaculum* were both increased in the EW group, while their levels were reduced by 2'-FL/LNnT supplementation (Fig. 6F). These findings suggest that while individual 2'-FL and LNnT treatments were ineffective, their combined action may restore gut microbiota homeostasis in EW mice through potential cross-feeding mechanisms among microbial communities.

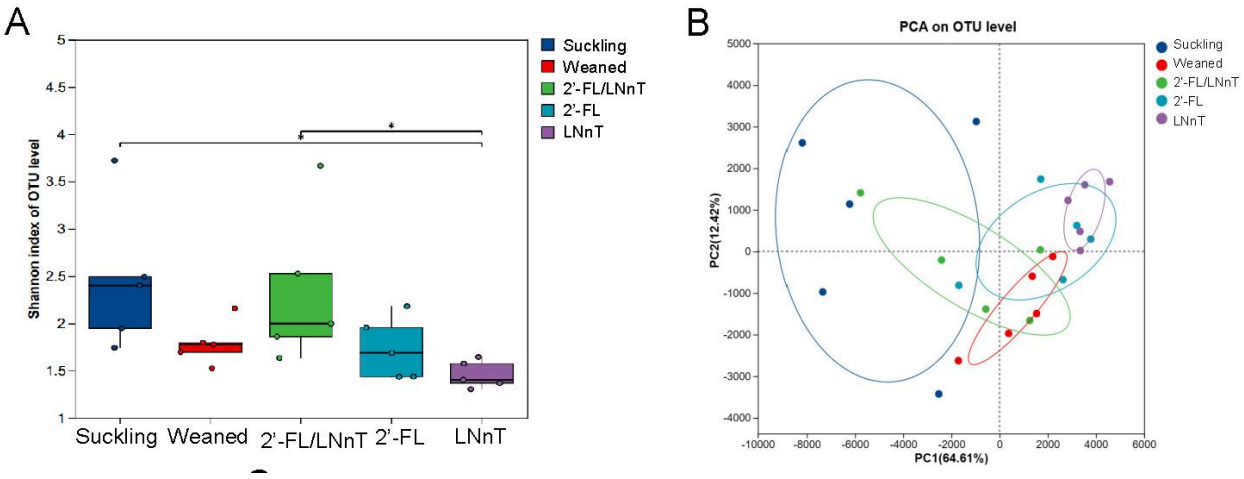

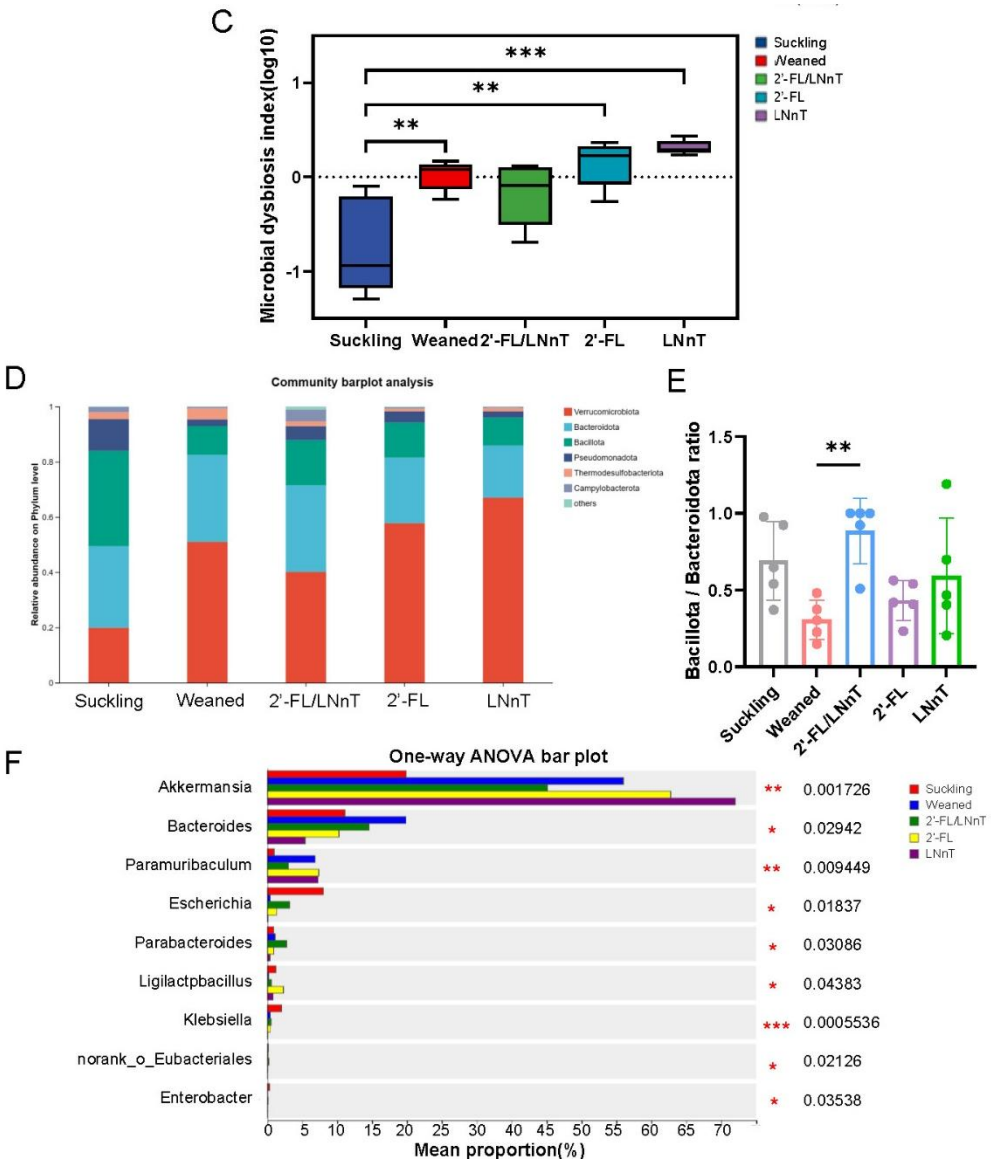

Figure 6. Effect of HMOs on the gut microbiota in early weaning (EW) mice. Mice were divided into five groups: (1) Normal suckling; (2) EW group; (3) EW + 2'-FL/LNnT (2'-FL + LNnT) group; (4) EW + 2'-FL group; and (5) EW + LNnT group. (A) The Shannon index of gut microbiota in 16S rDNA sequencing. (B) PCA plot at the OTU level. (C) The MDI was calculated for the five groups. (D) The microbial composition at the phylum level. (E) The ratio of Bacillota-to-Bacteroidota. n =5 per group. (F) Alterations in abundance of differential bacterial species across the five groups. *P < 0.05, **P < 0.01, ***P < 0.001.

3.6 2'-FL/LNnT attenuate intestinal epithelial damage in a microbiota-dependent manner

To determine if the gut microbiota mediates the protective effects of 2'-FL/LNnT on gut barrier integrity, we administered a broad-spectrum antibiotic cocktail to HMO-supplemented EW mice (ABX-EW mice, Fig. 7A), which resulted in an efficient depletion of the gut microbiota as confirmed via 16S rRNA gene qPCR (Fig. S3A). Notably, 2'-FL/LNnT treatment failed to ameliorate intestinal permeability in ABX-EW mice. Furthermore, jejunal histology appeared comparable across all groups, including suckling controls, EW mice, 2'-FL/LNnT-treated EW mice, and ABX-EW mice receiving 2'-FL/LNnT (Fig. 7B). Similarly, the villous height (Fig. 7C) and crypt depth (Fig. 7D) showed no statistical difference. Moreover, we evaluated the expression levels of tight junction-related protein and p-AMPK in the jejunum. We found a significant reduction in the expression of ZO-1, OCCLUDIN, and p-AMPK in both the EW and ABX +

2'-FL/LNnT groups compared with the suckling and 2'-FL/LNnT group (Fig.7E-F). qPCR analyses showed the mRNA levels of *Tjp1*, *Cldn1*, *Ocln*, and *Cdh1* were comparable between the EW mice and ABX-EW mice receiving 2'-FL/LNnT (Fig.7G).

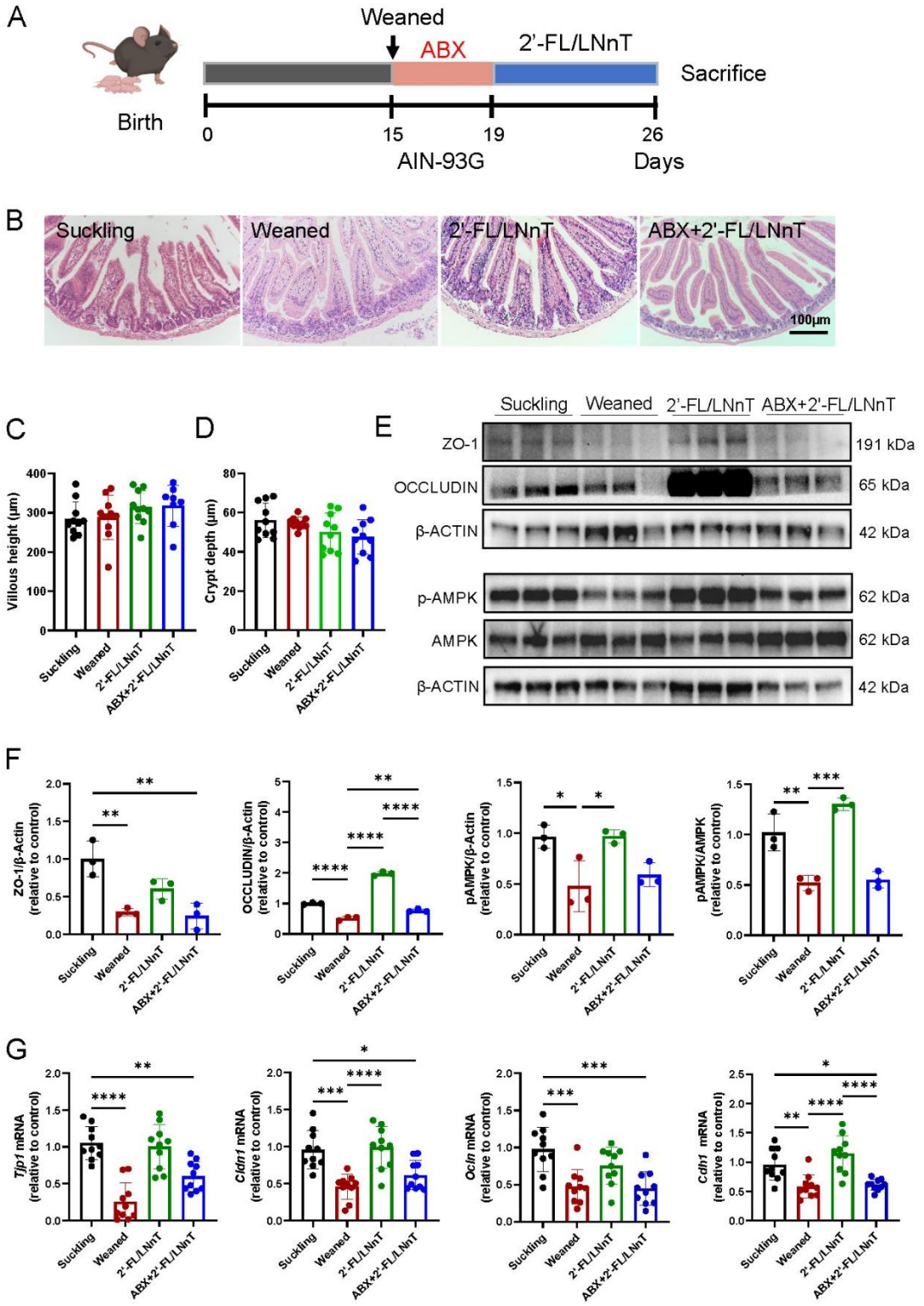

Figure 7. Impact of gut microbiota depletion on 2'-FL/LNnT-mediated protection against early weaning (EW)-induced intestinal dysfunction in mice. (A) Schematic diagram of the establishment of an antibiotic-induced gut microbiota depletion model (ABX mice). (B) H&E staining of jejunum in the suckling, EW, 2'-FL/LNnT, and ABX + 2'-FL/LNnT groups. (C) Villous height and (D) crypt depth were determined in mice. (E-F) Protein levels of ZO-1, OCCLUDIN, p-AMPK, and AMPK in the jejunum, as determined by western blotting (n =4 per group). (G) The mRNA levels of *Tjp1*, *Ocln*, and *Cldn1* in the jejunum, assessed by qPCR. **P* < 0.05, ***P* < 0.01, ****P* < 0.001, *****P* < 0.0001.

Next, we performed FMT experiments by transplanting the fecal supernatants from 2'-FL/LNnT-treated mice into ABX-treated EW mice (Fig.8A). The successful engraftment of donor microbiota was confirmed by tracking the levels *Akkermansia muciniphila*, an indicator species whose reduction in FMT groups mirrored the 2'-FL/LNnT treatment effect (Fig. S3B-D). Compared with the EW group, the 2'-FL/LNnT-FMT group significantly increased the jejunal villus height (Fig.8B-C), with no notable difference in crypt depth (Fig. 8B and D). The compromised gut barrier in the EW mice was significantly recovered after receiving gut microbiota from 2'-FL/LNnT-treated mice, as evidenced by the upregulated protein levels of ZO-1, OCCLUDIN, and p-AMPK (Fig. 8E-F), as well as mRNA levels of *Tjp1*, *Cldn1*, *Ocln*, and *Cdh1* (Fig.8G). These data suggest that the protective effects of 2'-FL/LNnT on intestinal barrier integrity can be transferred through gut microbiota.

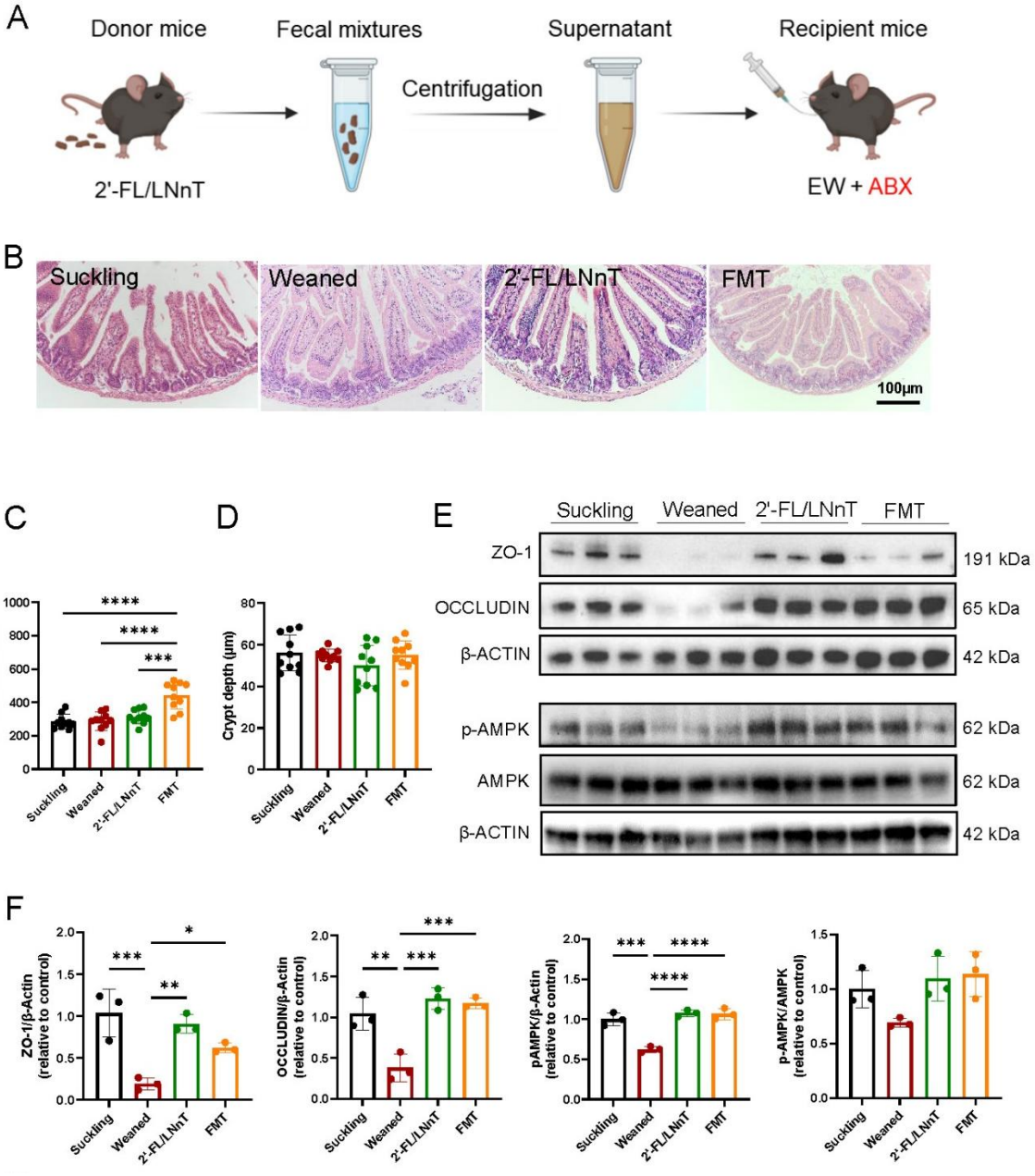

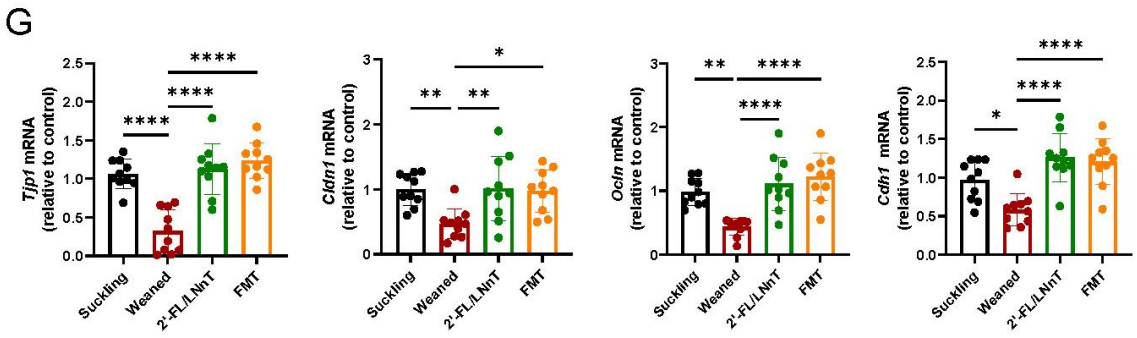

Figure 8. Fecal transplants of 2'-FL/LNnT exhibit protection against early weaning (EW)-induced intestinal dysfunction in mice. (A) Antibiotic-treated mice (ABX mice) received fecal microbiota transplantation (FMT) from 2'-FL/LNnT mice as donors for 7 days. (B) H&E staining on jejunum in the sucking, EW, 2'-FL/LNnT, and FMT groups. (C) Villous height and (D) crypt depth were determined in mice. (E-F) Protein levels of ZO-1, OCCLUDIN, p-AMPK, and AMPK in the jejunum, as determined by western blotting (n =4 per group). (D) The mRNA levels of *Tjp1*, *Ocln,* and *Cldn1* in the jejunum. $^{*}P < 0.05$, $^{**}P < 0.01$, $^{***}P < 0.001$, $^{****}P < 0.0001$.

Finally, we quantified fecal concentrations of SCFAs (acetic, propionic, isobutyric, butyric, isovaleric, and valeric acids) in all treatment groups. Interestingly, SCFA levels were comparable between the suckling and EW groups, whereas all HMO groups showed an upward trend. Furthermore, no significant differences in SCFA levels were observed among the 2'-FL/LNnT, 2'-FL, and LNnT groups. These results suggest that the synergistic effects of the 2'-FL/LNnT combination on the AMPK/SREBP1c pathway are independent of SCFA production (Fig. S4).

4. Discussion

EW is associated with abnormalities in intestinal epithelial function, thereby elevating the risk of gastrointestinal disease development. In this study, we established a mouse model of EW with isocaloric intake to investigate the pivotal role of 2'-FL and LNnT in mitigating intestinal dysfunction. Our data demonstrated that 2'-FL/LNnT activated the AMPK/SREBPs signaling pathway, leading to an upregulation of tight junction protein expression, which is crucial for maintaining intestinal barrier integrity. The protective effects of 2'-FL/LNnT in EW mice negated upon antibiotic administration and were transmissible via FMT.

In daily life, some breastfeeding mothers may need to cease nursing early due to individual circumstances, health conditions, or societal demands. Such early weaning is associated with increased risk of gastrointestinal diseases and can lead to intestinal atrophy in mammals. According to the precise age correlation between mice and humans, weaning at 14 days in mice is equivalent to weaning at around 3 months in humans [38]. We have developed an optimized early weaning (EW) mouse model based on established two-week-weaning protocols, incorporating stringent nutritional controls to minimize malnutrition-related confounders [24, 39]. A key advantage of our EW model over conventional systems is the use of isocaloric nutrition, which prevents malnutrition-associated metabolic disruptions and enables specific investigation of weaning-induced intestinal dysfunction.

The jejunum is the primary location for nutrient sensing and absorption. Previous studies using mouse and piglet weaning models have consistently shown that EW results in: (1) significant growth retardation, as evidenced by reduced body weight; (2) impaired intestinal development, characterized by decreased small

intestine length and diminished jejunal villus height; and (3) elevated pro-inflammatory mediators [25] [38]. Our results align with emerging evidence demonstrating that early weaning compromises jejunal barrier integrity. Contrary to previous reports, weaned mice receiving liquid diet supplementation exhibited comparable body weight, intestinal length, and histopathology to controls. This normalization of gross and microscopic parameters suggests that caloric supplementation prevents intestinal atrophy and restores homeostasis between enterocyte proliferation and apoptosis. Although liquid diet supplementation normalized growth metrics and ameliorated intestinal atrophy in weaned mice through restoration of enterocyte turnover, it did not correct EW-induced jejunal barrier dysfunction. Persistent epithelial hyperpermeability and sustained downregulation of tight junction proteins revealed a nutritionally resistant, segment-specific pathology (jejunum > ileum/colon).

Both 2’-FL and LNnT upregulate intestinal tight junction proteins, while 2’-FL providing additional protection against colitis through its triad of actions: prebiotic microbiota modulation, TLR4/NF-κB-mediated immunoregulation, and barrier enhancement via goblet cell stimulation and junctional protein induction [39]. Also, postoperative 2’-FL supplementation promotes mucosal adaptation in short bowel syndrome [40]. LNnT promotes intestinal epithelial growth and maturation during the early life of infant mice [23]. Here, we demonstrate that 2'-FL and LNnT significantly elevated tight junction protein levels and improved intestinal permeability through activation of the AMPK/SREBPs signaling pathway.

AMPK functions as a cellular energy sensor that can be activated by falling energy status [27]. It maintains cellular energy balance, regulates metabolism, responds to energy stress, and promotes tight junction assembly in intestinal epithelial cells [36, 41]. Importantly, AMPK plays a critical role in inhibiting fatty acid and cholesterol synthesis by directing phosphorylating and inhibiting the expression of acetyl-CoA carboxylase (ACC) and 3-hydroxy-3-methylglutaryl-CoA reductase (HMGCR), respectively [35]. As downstream targets of AMPK, SREBP1/2 were significantly upregulated in the EW group, suggesting that EW may enhance jejunal fatty acid and cholesterol synthesis, thereby impairing intestinal epithelial membrane integrity. Furthermore, AMPK downregulation was found to directly disrupt tight junction assembly. Notably, our results demonstrate that 2’-FL/LNnT significantly reduced the expression of both SREBF1 and SREBP2, along with their downstream target genes (*Fasn*, *Scd1*, *Acc1*), while HMOs supplementation had a synergistic effect.

Given that our in vitro experiments demonstrated that neither 2’-FL nor LNnT directly activated AMPK, and considering previous reports that their combination enhances gut barrier integrity via modulation of gut microbiota and SCFA production [18, 24], we further investigated their in vivo effects. Our results show that supplementation with 2’-FL and LNnT effectively restores gut dysbiosis and increased α-diversity in EW mice, resulting in a microbial profile resembling that of control animals. However, the synergistic benefits of the 2’-FL/LNnT combination on gut barrier function do not appear to be mediated by changes in SCFA levels. Instead, we speculate that these oligosaccharides may directly interact with host epithelial or immune receptors, modulate the gut microbiota through mechanisms beyond SCFA production, or promote the

synthesis of other functional microbial metabolites. In support of this notion, Zhu, et al. [42] reported that cognitive improvement was associated with gut microbiota modulation and elevated 5-hydroxytryptophan levels—an example of a non-SCFA-mediated mechanism. Therefore, future studies should focus on clarifying the individual and combined effects of 2'-FL and LNnT on specific microbial taxa and their metabolic outputs to elucidate the precise basis of their synergistic action.

While our study elucidates the beneficial effects of 2'-FL/LNnT in a murine model, the clinical translatability of these findings to EW infants requires further validation. Caution should be exercised when extrapolating these results due to inherent interspecies differences in gut physiology and microbiota composition between mice and humans. Another limitation is that the specific taxa through which 2'-FL/LNnT mediate the intestinal epithelial tight junctions remain undetermined. Future studies are warranted to identify the functional microbiota and validate their roles in intestinal barrier function.

In conclusion, we demonstrate that 2'-FL and LNnT, by reshaping the gut microbiota and activating the AMPK/SREBPs signaling pathway, synergistically enhance tight junction protein expression and improve intestinal barrier function. This study provides potential therapeutic strategies for addressing intestinal barrier dysfunction and gut dysbiosis in the context of EW.

Acknowledgement

We are grateful to Dr. Yang Liu for his assistance with the animal experiments and Yajie Zhang for manuscript editing. This study was supported by grants from Shanghai Key Laboratory of Pediatric Gastroenterology and Nutrition (2018ZDPTJD03) and National Natural Science Foundation of China (82401034). The graphical abstract is created with Biorender.com.

Ethical statement

All animal experiments were conducted humanely and were approved by the Animal Care and Use Committee of Xinhua Hospital Affiliated to Shanghai Jiao Tong University School of Medicine (Approval No. XHEC-F-2025-058).

References

[1] K. North, M. Gao, G. Allen, et al., Breastfeeding in a Global Context: Epidemiology, Impact, and Future Directions, Clin Ther. 2022;44(2):228-244. https://dx.doi.org/10.1016/j.clinthera.2021.11.017.

[2] G. Lack, M. Penagos. Early feeding practices and development of food allergies, Nestle Nutr Workshop Ser Pediatr Program. 2011;68:169-183; discussion 183-166. https://dx.doi.org/10.1159/000325855.

[3] B.L. Horta, C. Loret de Mola, C.G. Victora. Long-term consequences of breastfeeding on cholesterol, obesity, systolic blood pressure and type 2 diabetes: a systematic review and meta-analysis, Acta Paediatr. 2015;104(467):30-37. https://dx.doi.org/10.1111/apa.13133.

[4] S. Ajmal, L. Ajmal, M. Ajmal, et al., Association of Malnutrition With Weaning Practices Among Infants in Pakistan, Cureus. 2022;14(11):e31018. https://dx.doi.org/10.7759/cureus.31018.

[5] L.M. Lamberti, C.L. Fischer Walker, A. Noiman, et al., Breastfeeding and the risk for diarrhea morbidity and mortality, BMC Public Health. 2011;11 Suppl 3(Suppl 3):S15. https://dx.doi.org/10.1186/1471-2458-11-s3-s15.

[6] F.C. Neiva, D.M. Cattoni, J.L. Ramos, et al., [Early weaning: implications to oral motor development], J Pediatr (Rio J). 2003;79(1):7-12.

[7] A. Fawzy, S. Arpadi, C. Kankasa, et al., Early weaning increases diarrhea morbidity and mortality among uninfected children born to HIV-infected mothers in Zambia, J Infect Dis. 2011;203(9):1222-1230. https://dx.doi.org/10.1093/infdis/jir019.

[8] C. Onyango-Makumbi, D. Bagenda, A. Mwatha, et al., Early weaning of HIV-exposed uninfected infants and risk of serious gastroenteritis: Findings from two perinatal HIV prevention trials in Kampala, Uganda, J Acquir Immune Defic Syndr. 2010;53(1):20-27. https://dx.doi.org/10.1097/QAI.0b013e3181bdf68e.

[9] H. Siljander, E. Jason, T. Ruohtula, et al., Effect of Early Feeding on Intestinal Permeability and Inflammation Markers in Infants with Genetic Susceptibility to Type 1 Diabetes: A Randomized Clinical Trial, J Pediatr. 2021;238:305-311.e303. https://dx.doi.org/10.1016/j.jpeds.2021.07.042.

[10] L. Shenhav, K. Fehr, M.E. Reyna, et al., Microbial colonization programs are structured by breastfeeding and guide healthy respiratory development, Cell. 2024;187(19):5431-5452.e5420. https://dx.doi.org/10.1016/j.cell.2024.07.022.

[11] B. Xia, R. Zhong, Q. Meng, et al., Multi-omics unravel the compromised mucosal barrier function linked to aberrant mucin O-glycans in a pig model, Int J Biol Macromol. 2022;207:952-964. https://dx.doi.org/10.1016/j.ijbiomac.2022.03.173.

[12] C.H. Hu, K. Xiao, Z.S. Luan, et al., Early weaning increases intestinal permeability, alters expression of cytokine and tight junction proteins, and activates mitogen-activated protein kinases in pigs, J Anim Sci. 2013;91(3):1094-1101. https://dx.doi.org/10.2527/jas.2012-5796.

[13] O. Ballard, A.L. Morrow. Human milk composition: nutrients and bioactive factors, Pediatr Clin North Am. 2013;60(1):49-74. https://dx.doi.org/10.1016/j.pcl.2012.10.002.

[14] M. Elwakiel, J.A. Hageman, W. Wang, et al., Human Milk Oligosaccharides in Colostrum and Mature Milk of Chinese Mothers: Lewis Positive Secretor Subgroups, J Agric Food Chem. 2018;66(27):7036-7043. https://dx.doi.org/10.1021/acs.jafc.8b02021.

[15] Z. Tang, Y. Yang, M. Yang, et al., Elucidating the modulatory role of dietary hydroxyproline on the integrity and functional performance of the intestinal barrier in early-weaned piglets: A comprehensive analysis of its interplay with the gut microbiota and metabolites, Int Immunopharmacol. 2024;134:112268. https://dx.doi.org/10.1016/j.intimp.2024.112268.

[16] P.P.J. Jackson, A. Wijeyesekera, R.A. Rastall. Determining the metabolic fate of human milk oligosaccharides: it may just be more complex than you think?, Gut Microbiome (Camb). 2022;3:e9. https://dx.doi.org/10.1017/gmb.2022.8.

[17] G. Puccio, P. Alliet, C. Cajozzo, et al., Effects of Infant Formula With Human Milk Oligosaccharides on Growth and Morbidity: A Randomized Multicenter Trial, J Pediatr Gastroenterol Nutr. 2017;64(4):624-631. https://dx.doi.org/10.1097/mpg.0000000000001520.

[18] K.M. Tonon, M.K. Salgaço, V. Mesa, et al., Infant formula with 2′-FL + LNnT positively modulates the infant gut microbiome: An in vitro study using human intestinal microbial ecosystem model, International Dairy Journal. 2023;139:105558. https://dx.doi.org/https://doi.org/10.1016/j.idairyj.2022.105558.

[19] M.S. Gold, P.J. Quinn, D.E. Campbell, et al., Effects of an Amino Acid-Based Formula Supplemented with Two Human Milk Oligosaccharides on Growth, Tolerability, Safety, and Gut Microbiome in Infants with Cow's Milk Protein Allergy, Nutrients. 2022;14(11). https://dx.doi.org/10.3390/nu14112297.

[20] Y. Zhu, L. Wan, W. Li, et al., Recent advances on 2'-fucosyllactose: physiological properties, applications, and production approaches, Crit Rev Food Sci Nutr. 2022;62(8):2083-2092. https://dx.doi.org/10.1080/10408398.2020.1850413.

[21] P. Zhang, Y. Zhu, Z. Li, et al., Recent Advances on Lacto-N-neotetraose, a Commercially Added Human Milk Oligosaccharide in Infant Formula, J Agric Food Chem. 2022;70(15):4534-4547. https://dx.doi.org/10.1021/acs.jafc.2c01101.

[22] J. Li, Y. Wei, C. Liu, et al., 2'-Fucosyllactose restores the intestinal mucosal barrier in ulcerative colitis by inhibiting STAT3 palmitoylation and phosphorylation, Clin Nutr. 2024;43(2):380-394. https://dx.doi.org/10.1016/j.clnu.2023.12.011.

[23] J. Liao, M. Wang, H. Li, et al., Human Milk Oligosaccharide LNnT Promotes Intestinal Epithelial Growth and Maturation During the Early Life of Infant Mice, J Agric Food Chem. 2025;73(11):6678-6690. https://dx.doi.org/10.1021/acs.jafc.4c10055.

[24] B. Berger, N. Porta, F. Foata, et al., Linking Human Milk Oligosaccharides, Infant Fecal Community Types, and Later Risk To Require Antibiotics, mBio. 2020;11(2). https://dx.doi.org/10.1128/mBio.03196-19.

[25] J. Tian, Y. Li, X. Bao, et al., Early weaning causes small intestinal atrophy by inhibiting the activity of intestinal stem cells: involvement of Wnt/β-catenin signaling, Stem Cell Res Ther. 2023;14(1):65. https://dx.doi.org/10.1186/s13287-023-03293-9.

[26] P.G. Reeves, F.H. Nielsen, G.C. Fahey, Jr., AIN-93 purified diets for laboratory rodents: final report of the American Institute of Nutrition ad hoc writing committee on the reformulation of the AIN-76A rodent diet, J Nutr. 1993;123(11):1939-1951. https://dx.doi.org/10.1093/jn/123.11.1939.

[27] X. Feng, M. Wang, S. Wen, et al., Lactiplantibacillus plantarum P101 Alleviated Alcohol-Induced Hepatic Lipid Accumulation in Mice via AMPK Signaling Pathway: Gut Microbiota and Metabolomics Analysis, Probiotics Antimicrob Proteins. 2024. https://dx.doi.org/10.1007/s12602-024-10373-6.

[28] P. Gu, R. Wei, R. Liu, et al., Aging-induced Alternation in the Gut Microbiota Impairs Host Antibacterial Defense, Adv Sci (Weinh). 2025;12(12):e2411008. https://dx.doi.org/10.1002/advs.202411008.

[29] L. Hidalgo-Garcia, J.A. Molina-Tijeras, F. Huertas-Peña, et al., Intestinal mesenchymal cells regulate immune responses and promote epithelial regeneration in vitro and in dextran sulfate sodium-induced experimental colitis in mice, Acta Physiol (Oxf). 2021;233(2):e13699. https://dx.doi.org/10.1111/apha.13699.

[30] A. Kechin, U. Boyarskikh, A. Kel, et al., cutPrimers: A New Tool for Accurate Cutting of Primers from Reads of Targeted Next Generation Sequencing, J Comput Biol. 2017;24(11):1138-1143. https://dx.doi.org/10.1089/cmb.2017.0096.

[31] D. Kim, B. Langmead, S.L. Salzberg. HISAT: a fast spliced aligner with low memory requirements, Nat Methods. 2015;12(4):357-360. https://dx.doi.org/10.1038/nmeth.3317.

[32] M.I. Love, W. Huber, S. Anders. Moderated estimation of fold change and dispersion for RNA-seq data with DESeq2, Genome Biol. 2014;15(12):550. https://dx.doi.org/10.1186/s13059-014-0550-8.

[33] M. Kanehisa, M. Furumichi, Y. Sato, et al., KEGG: integrating viruses and cellular organisms, Nucleic Acids Res. 2021;49(D1):D545-d551. https://dx.doi.org/10.1093/nar/gkaa970.

[34] L. Du, K. Zhang, L. Liang, et al., Multi-omics analyses of the gut microbiota and metabolites in children with metabolic dysfunction-associated steatotic liver disease, mSystems. 2025;10(4):e0114824. https://dx.doi.org/10.1128/msystems.01148-24.

[35] G.R. Steinberg, D.G. Hardie. New insights into activation and function of the AMPK, Nat Rev Mol Cell Biol. 2023;24(4):255-272. https://dx.doi.org/10.1038/s41580-022-00547-x.

[36] P. Rowart, J. Wu, M.J. Caplan, et al., Implications of AMPK in the Formation of Epithelial Tight Junctions, Int J Mol Sci. 2018;19(7). https://dx.doi.org/10.3390/ijms19072040.

[37] Y. Li, S. Xu, M.M. Mihaylova, et al., AMPK phosphorylates and inhibits SREBP activity to attenuate hepatic steatosis and atherosclerosis in diet-induced insulin-resistant mice, Cell Metab. 2011;13(4):376-388. https://dx.doi.org/10.1016/j.cmet.2011.03.009.

[38] S. Cao, L. Hou, L. Sun, et al., Intestinal morphology and immune profiles are altered in piglets by early-weaning, Int Immunopharmacol. 2022;105:108520. https://dx.doi.org/10.1016/j.intimp.2022.108520.

[39] T. Chen, C. Wang, C. Nie, et al., Galactooligosaccharide or 2'-Fucosyllactose Modulates Gut Microbiota and Inhibits LPS/TLR4/NF-κB Signaling Pathway to Prevent DSS-Induced Colitis Aggravated by a High-Fructose Diet in Mice, J Agric Food Chem. 2023;71(24):9349-9360. https://dx.doi.org/10.1021/acs.jafc.2c08814.

[40] E.A. Mezoff, J.A. Hawkins, N.J. Ollberding, et al., The human milk oligosaccharide 2'-fucosyllactose augments the adaptive response to extensive intestinal, Am J Physiol Gastrointest Liver Physiol. 2016;310(6):G427-438. https://dx.doi.org/10.1152/ajpgi.00305.2015.

[41] S. Olivier, J. Leclerc, A. Grenier, et al., AMPK Activation Promotes Tight Junction Assembly in Intestinal Epithelial Caco-2 Cells, Int J Mol Sci. 2019;20(20). https://dx.doi.org/10.3390/ijms20205171.

[42] L. Zhu, Z. Zhang, T. Luo, et al., Cognitive and behavioral benefits of 2'-fucosyllactose in growing mice: the roles of 5-hydroxytryptophan and gut microbiota, Microbiome. 2025;13(1):97. https://dx.doi.org/10.1186/s40168-025-02094-x.